

RSC Advances



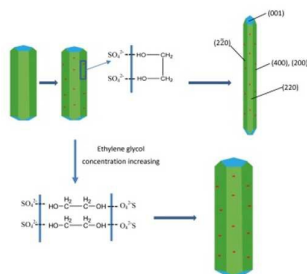
This is an *Accepted Manuscript*, which has been through the Royal Society of Chemistry peer review process and has been accepted for publication.

Accepted Manuscripts are published online shortly after acceptance, before technical editing, formatting and proof reading. Using this free service, authors can make their results available to the community, in citable form, before we publish the edited article. This *Accepted Manuscript* will be replaced by the edited, formatted and paginated article as soon as this is available.

You can find more information about *Accepted Manuscripts* in the [Information for Authors](#).

Please note that technical editing may introduce minor changes to the text and/or graphics, which may alter content. The journal's standard [Terms & Conditions](#) and the [Ethical guidelines](#) still apply. In no event shall the Royal Society of Chemistry be held responsible for any errors or omissions in this *Accepted Manuscript* or any consequences arising from the use of any information it contains.

A facile ethylene glycol-assisted hydrothermal method was developed to synthesis HH whiskers with high aspect ratios.





Journal Name

ARTICLE

Effect of Ethylene Glycol on Hydrothermal Formation of Calcium Sulfate Hemihydrate Whiskers with High Aspect Ratios

Wenpeng Zhao, Yumin Wu, Jun Xu, Chuanhui Gao

Received 00th January 20xx,
Accepted 00th January 20xx

DOI: 10.1039/x0xx00000x

www.rsc.org/

Abstract : The effect of ethylene glycol on hydrothermal formation of calcium sulfate hemihydrate (HH) with high aspect ratios was investigated in this work. HH whiskers with a preferential growth along the *c* axis and an average aspect ratio up to 400 were synthesized using oyster shells as raw materials in the presence of 3.76×10^{-3} mol·L⁻¹ ethylene glycol. The preferential adsorption of ethylene glycol on the negative (200), (400), and (220) facets was confirmed by IR, XRD, XPS, and zeta potential measurements. The experimental results indicated that the adsorption and doping of ethylene glycol promoted the 1-D growth of HH whiskers, leading to the formation of whiskers with high aspect ratios.

1. Introduction

One-dimensional (1-D) materials, such as rods [1], wires [2, 3, 4], whiskers [5], and tubes [6], have drawn much attention due to their excellent physical-chemical properties and practical applications in electronics, chemical engineering and superconductivity. The mechanical properties of 1-D calcium sulfate whiskers were usually improved with an increase in the aspect ratio [7-9]. According to the continuum theory [8], the modulus of elasticity (*E*) of homogeneous rod-shape increases with the increasing aspect ratios.

Calcium sulfate whiskers with a high aspect ratio, owing to its good thermal stability, chemical resistance, almost perfect structure, low cost, and possessing high strength and stiffness [10], are widely used as a reinforcing agent in polymer, rubber, ceramic composites and so on [11-17]. Being different from conventional fillers or reinforcement, such as kaolin, calcium sulfate, carbon fibers etc, calcium sulfate whisker is considered to be an attractive material which combined inorganic fillers and reinforced fibers [18]. It was reported [19] [20] that calcium sulfate was considered as PLA fillers, tensile and impact properties proved to be maintained at a very acceptable level at filler content as high as 50 wt%, the presence of 15 wt % of calcium sulfate whiskers in the polycaprolactone composite led to the increase of 21% in flexural strength and 22% in the impact strength, the tensile strength and the elongation of polypropylene (PP) reached up to 39.18 MPa and 125.4%, respectively, after filling 5 wt % of calcium sulfate whiskers.

The aspect ratio of calcium sulfate hemihydrate whiskers can be promoted by many methods, including the activation of the raw materials, the alteration of the process parameters, the use of the organic and inorganic additives, and so on. For example, calcium sulfate hemihydrate whiskers with an aspect ratio up to 325 were prepared by hydrothermal treatment of the active calcium sulfate dehydrate (calcination of the commercial CaSO₄·2H₂O at 150°C for 6.0 h followed by hydration at room temperature for 1.0 h) precursor [21], the hydroxyl groups of glycerol adsorbed and occupied the vacancies of Ca sites on (001) plane of CaSO₄·0.5H₂O whiskers, and formed hydrogen bond with Ca on (100) let to increase the aspect ratios from 29 to 118 in the presence of 10 %- 100 % glycerol [22], the aspect ratio of calcium sulfate hemihydrate whiskers up to 370 were synthesized using hydrothermal treatment of CaSO₄·2H₂O precursor in the presence of 1.97×10^{-3} mol·L⁻¹ MgCl₂ [20]. The preferential adsorption and inhibition of cetyltrimethyl ammonium bromide (CTAB) on the side facets and sodium dodecyl sulfonate (SDS) on the top facets of calcium sulfate hemihydrate whiskers led to the increase in the aspect ratios from 2-7 to 180-250 in the reversed micro-emulsion system [23].

A facile method was developed to synthesize calcium sulfate hemihydrate whiskers with high aspect ratios by hydrothermal treatment using oyster shells as raw materials in the presence of minor amount of ethylene glycol. The adsorption of ethylene glycol in the hydrothermal formation of calcium sulfate hemihydrate whiskers was revealed, and the corresponding mechanisms were studied.

2. Experimental

2.1. Experiment Procedure

Commercial chemicals with analytical grade were used in the experiments. calcium sulfate dihydrate, synthesized from oyster shells, mixed with deionized water and minor amount

^a Address 53 Zhengzhou Road, Qingdao 266042, (China).

^b Address 53 Zhengzhou Road, Qingdao 266042, (China).

^c Address 53 Zhengzhou Road, Qingdao 266042, (China).

† Footnotes relating to the title and/or authors should appear here.

Electronic Supplementary Information (ESI) available: [details of any

supplementary information available should be included here]. See

DOI: 10.1039/x0xx00000x

of ethylene glycol with a purity of 98.0% at room temperature to get the suspensions containing 1.0–5.0 wt % calcium sulfate dihydrate and 0 to $5.47 \times 10^{-3} \text{ mol}\cdot\text{L}^{-1}$ ethylene glycol. The slurries were then treated under hydrothermal condition (140 °C, 4.0 h), filtrated, and dried at 105 °C for 6.0 h.

2.2. Characterization.

The morphology of the samples were characterized with the field-emission scanning electron microscopy (SEM, JEOL JSM-6, Japan), the high-resolution transmission electron microscopy (HRTEM, JEM-2100, Japan) equipped with the selected area electron diffraction (SAED). The structures of the samples were identified by powder X-ray diffractometer (XRD, Rigaku D-MAX-2500/PC, Japan) using $\text{Cu K}\alpha 1$ radiation ($\lambda=1.54178 \text{ \AA}$), with a scanning rate of 5° min^{-1} and scanning 2θ range of 5 to 90° . X-ray photoelectron spectrometer (XPS, Thermo ESCALAB 250Xi, USA) was employed to examine the surface adsorption of ethylene glycol by using an $\text{Al K}\alpha$ X-ray source operated at 150W. The IR spectra was obtained by BRUKER TENSOR-27 Fourier transform infrared (FTIR) spectrophotometer using a KBr Pellet. The surface electric potential was measured with the Zeta Potential (Zetasize NanoZS-90, Malvern Instruments) in the pH range of 2.0 to 13.0. The average diameters and the lengths of the whiskers for each sample were estimated by direct measuring about 200 whiskers from the typical FESEM images with the magnifications of 100–5000.

3. Results and discussion

3.1. Effect of Ethylene Glycol on the Formation of Calcium Sulfate Hemihydrate (HH) Whiskers

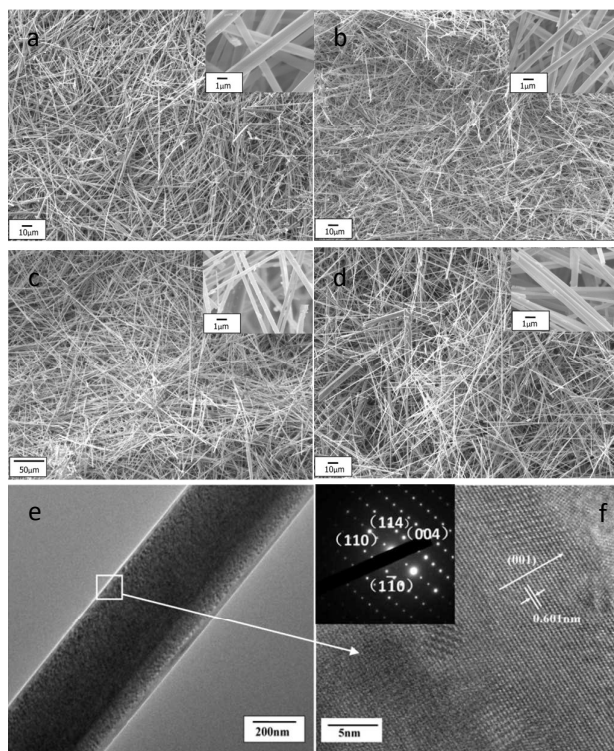


Figure 1. Influence of ethylene glycol on the morphology of HH whiskers (a-f): (a) 0, (b) $1.09 \times 10^{-3} \text{ mol}\cdot\text{L}^{-1}$, (c, e, f) $3.76 \times 10^{-3} \text{ mol}\cdot\text{L}^{-1}$, (d) $5.47 \times 10^{-3} \text{ mol}\cdot\text{L}^{-1}$

The influence of ethylene glycol on morphology of the hydrothermal products formed at 140 °C is shown in Figure 1, the distributions of the diameters and the aspect ratios are shown in Figure 2. HH whiskers with a length of 50–280 μm , an average width of $0.93 \mu\text{m}$, and an average aspect ratio of about 132 were synthesized in the absence of ethylene glycol (Figure 1a). As the ethylene glycol concentration increased from $1.09 \times 10^{-3} \text{ mol}\cdot\text{L}^{-1}$ to $5.47 \times 10^{-3} \text{ mol}\cdot\text{L}^{-1}$, the lengths of the whiskers first increased from 80–320 μm to 150–400 μm , and then declined to 90–320 μm , and the average diameter first decreased from $0.8 \mu\text{m}$ to $0.53 \mu\text{m}$, then rose to $0.97 \mu\text{m}$ (Figure 1b, c, d). The average aspect ratio of the whiskers reached up to 400 in the presence of $3.76 \times 10^{-3} \text{ mol}\cdot\text{L}^{-1}$ ethylene glycol.

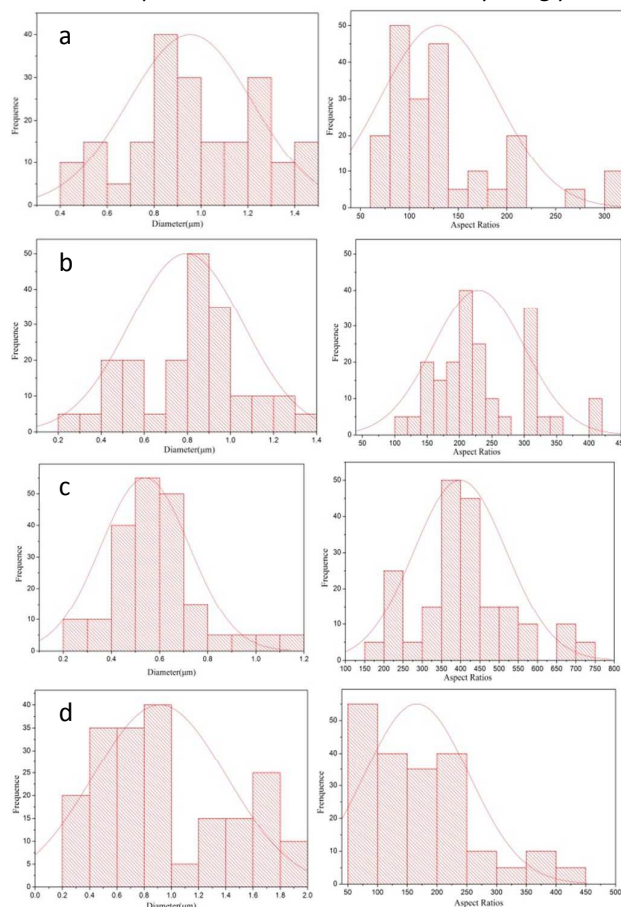


Figure 2. Diameter and aspect ratio distributions of HH whiskers: (a) 0, (b) $1.09 \times 10^{-3} \text{ mol}\cdot\text{L}^{-1}$, (c) $3.76 \times 10^{-3} \text{ mol}\cdot\text{L}^{-1}$, (d) $5.47 \times 10^{-3} \text{ mol}\cdot\text{L}^{-1}$

TEM, SAED, and high-resolution TEM (HRTEM) have been performed to investigate the morphology and structure of the whisker further. Figure 1e exhibits the whisker in the morphology of the long rod, and inset SAED pattern shown in Figure 1f can be indexed to the $[1\bar{1}0]$ zone axis of whisker. The indexes of the spots in the SAED pattern indicate that the whisker is single-crystalline and grows along the (001) direction. The fringe spacing of 0.601 nm in the HRTEM image (Figure 1f) corresponds to the (002) plane ($d(002)=0.599 \text{ nm}$), further indicating the preferential growth along the (001)

direction.

The XRD patterns are shown in Figure 3. Al_2O_3 was used as the reference sample to eliminate the experimental deviation. The same location of Al_2O_3 sample ($2\theta=35.124^\circ$) in all cases confirmed the accuracy of the XRD spectra. All of the XRD peaks were attributed to the sole existence of HH. Most of the occurred planes as (200), (220), and (400) were parallel to the *c* axis, reconfirming the preferential growth of the HH whiskers along *c* axis.

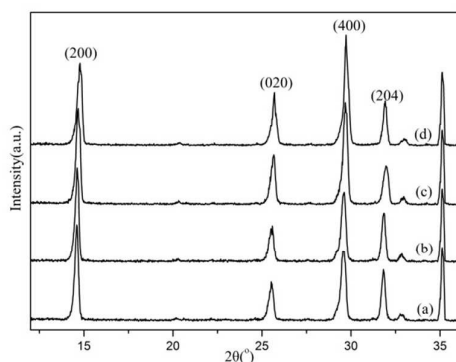


Figure 3. Influence of ethylene glycol on XRD patterns of HH whiskers: (a) 0, (b) $1.09 \times 10^{-3} \text{ mol}\cdot\text{L}^{-1}$, (c) $3.76 \times 10^{-3} \text{ mol}\cdot\text{L}^{-1}$, (d) $5.47 \times 10^{-3} \text{ mol}\cdot\text{L}^{-1}$

3.2. Growth Mechanism of HH Whiskers with High Aspect Ratio

Figure 4 shows the influence of ethylene glycol on the peak shift on the XRD pattern of the HH whiskers. The presence of 0, $1.09 \times 10^{-3} \text{ mol}\cdot\text{L}^{-1}$, $5.47 \times 10^{-3} \text{ mol}\cdot\text{L}^{-1}$, and $3.76 \times 10^{-3} \text{ mol}\cdot\text{L}^{-1}$ ethylene glycol led to the shift of 2θ for (200) peaks from 14.602° to 14.621° , 14.675° , and 14.772° , (220) peaks from 25.531° to 25.592° , 25.682° , and 25.696° , and (400) peaks from 29.590° to 29.611° , 29.682° , and 29.723° , respectively. The phenomena illustrated the possible absorption of ethylene glycol on those planes. The absorption of ethylene glycol on the (200), (220), and (400) may inhibit the growth of the whiskers along the radial direction and promote the 1-D growth of the whiskers along the *c* axis, leading to the formation of HH whiskers with high aspect ratios.

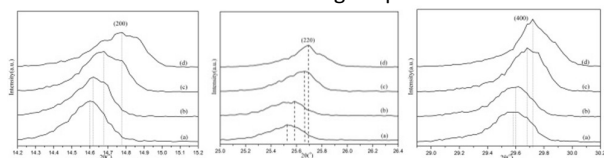


Figure 4. Influence of ethylene glycol on peak shift of XRD patterns of HH whiskers: (a) 0, (b) $1.09 \times 10^{-3} \text{ mol}\cdot\text{L}^{-1}$, (c) $3.76 \times 10^{-3} \text{ mol}\cdot\text{L}^{-1}$, (d) $5.47 \times 10^{-3} \text{ mol}\cdot\text{L}^{-1}$

The zeta potentials have been performed to confirm the adsorption of ethylene glycol on the surface of HH whiskers. The influence of ethylene glycol on the zeta potentials of HH whiskers is shown in Figure 5. The data in curve a indicated the absence of ethylene glycol, and the zeta potential declined from -8.32 to -21.6 mV as pH increased from 2.1 to 10.1, indicating that the whisker surface were negatively charged under the experimental conditions. The data in curves b, c, and d showed that the presence of ethylene glycol led to increase in the zeta potentials, while the surfaces of HH whiskers were still negatively charged. The increase in the zeta potentials with the increase in ethylene glycol concentration indicated

that the adsorption of ethylene glycol on the surface of HH whiskers.

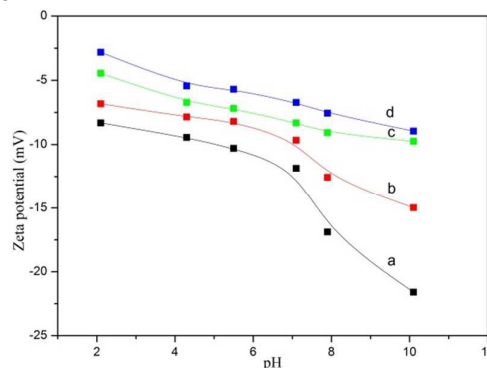


Figure 5. Influence of ethylene glycol on zeta potential of HH whiskers: (a) 0, (b) $1.09 \times 10^{-3} \text{ mol}\cdot\text{L}^{-1}$, (c) $3.76 \times 10^{-3} \text{ mol}\cdot\text{L}^{-1}$, (d) $5.47 \times 10^{-3} \text{ mol}\cdot\text{L}^{-1}$

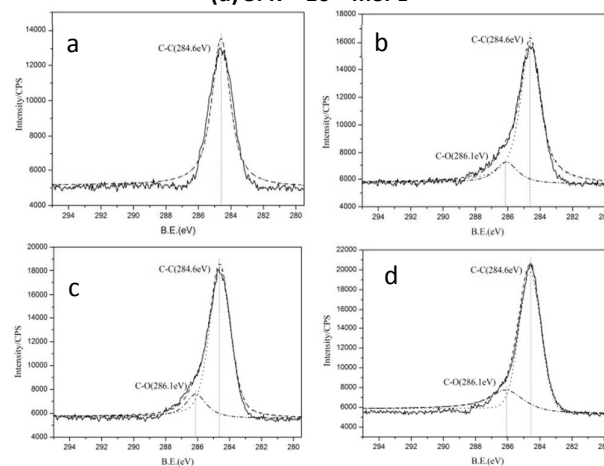


Figure 6. Influence of ethylene glycol on C1s XPS spectra of HH whiskers: (a) 0, (b) $1.09 \times 10^{-3} \text{ mol}\cdot\text{L}^{-1}$, (c) $3.76 \times 10^{-3} \text{ mol}\cdot\text{L}^{-1}$, (d) $5.47 \times 10^{-3} \text{ mol}\cdot\text{L}^{-1}$

The XPS was employed to further confirm the adsorption of ethylene glycol on the surface of HH whiskers. Figure 6a shows the C1s spectra of blank sample, there is no other peak except the main C-C peak at 284.6 eV, indicating there is no carbon functional group on the surface of HH whiskers. As shown in Figure 6b, c, and d, aside from the main C-C peak at around 284.6 eV, additional photoemission present at higher binding energies indicates the presence of carbon atoms bonded to other functional groups. The binding energy peak at 286.1 eV is attributed to the C atoms in hydroxyl and epoxy/ether groups (C-O) [24], reconfirming the adsorption of ethylene glycol on the surface of HH whiskers.

Table 1. Atomic Concentrations Calculated from XPS Experimental Data

| sample | concentration of carbon (atomic %) |
|--------|------------------------------------|
| a | NA |
| b | 2.41 |
| c | 4.74 |
| d | 5.45 |

On the basis of these XPS results, the C1s, O1s, Ca2s, and S2s peak areas were determined. The peak areas and use of atomic sensitivity factors provide the atomic concentration, providing a quantitative measure of the extent of element and

the concentration values of carbon in ethylene glycol given in table 1 were based on this [25]. Compared with the blank experiment, 2.41, 4.74 and 5.45% of carbon were detected in the presence of 1.09×10^{-3} , 3.76×10^{-3} , 5.47×10^{-3} mol·L⁻¹ ethylene glycol, respectively.

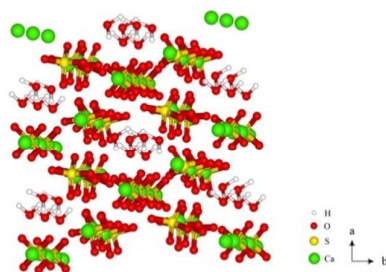


Figure 7. Structure of HH whiskers along the *c*-axis direction

The amount of ethylene glycol adsorbed on the surface of whiskers plays key roles in formation of HH whiskers with high aspect ratio. We believe that hydrogen bonds were formed between hydroxy and SO₄²⁻ on the HH whiskers surface are responsible for the high aspect ratio. The surface interactions are closely associated with the structure of HH. Figure 7 shows the molecular structure of CaSO₄·0.5H₂O deduced by Material Studio 5.0 software [26]. The crystal lattice of HH consists of repeating, ionically bonded Ca and SO₄ atoms in chains of –Ca–SO₄–Ca–SO₄– in which each S atom is covalently bonded to four O atoms that form a tetrahedral corner [27, 28]. These chains are hexagonally arranged and form a framework parallel to the *c* axis with continuous channels with diameter of about 4.5Å, where one water molecule is attached to every two calcium sulfate molecules [29]. The structure presents a denser distribution of SO₄²⁻ ions on the side facets of [220], [200], and [400] and a denser distribution of Ca²⁺ ions on the top facets [001]. The preferential adsorption of ethylene glycol molecules to the [200], [220], and [400] facets of HH whiskers will lower the surface free energy of these facets, which favored the 1-D growth of HH whiskers along the *c* axis.

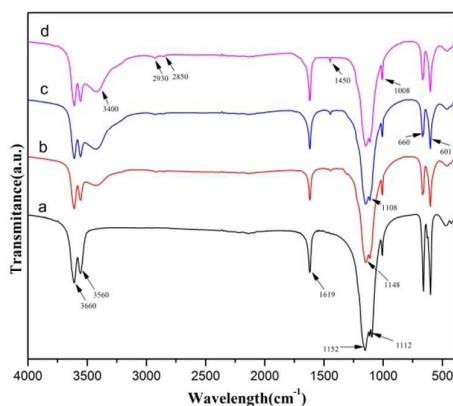


Figure 8. FTIR spectra of HH whisker formed in the present of ethylene glycol: (a) 0, (b) 1.09×10^{-3} mol·L⁻¹, (c) 3.76×10^{-3} mol·L⁻¹, (d) 5.47×10^{-3} mol·L⁻¹

To confirm the hydrogen bonds between ethylene glycol and SO₄²⁻, the Fourier transform infrared (FTIR) spectra of HH whiskers were recorded as shown in Figure 8. The bands at 3560, 3660 cm⁻¹ and 1619 cm⁻¹ associated with crystal water molecule combined on CaSO₄ [30, 31], the band at 1008 cm⁻¹

can be assigned to ν_1 SO₄²⁻ stretching, the bands at 1112 and 1152 cm⁻¹ can be assigned to ν_3 SO₄²⁻ stretching, and the bands at 601 and 660 cm⁻¹ can be assigned to ν_4 SO₄²⁻ stretching. The characteristic absorption peaks of HH further verify that all of the samples are composed of HH. Two bands are observed in the region of 2800–3000cm⁻¹ and are assigned to the asymmetric (2930 cm⁻¹) and symmetric (2850cm⁻¹) stretching vibration of CH₂, and its bending bond at 1450 cm⁻¹, the band at 3400 cm⁻¹ is ascribed to the stretching of O–H in ethylene glycol, which indicate that ethylene glycol is present on the HH whiskers. The bands at 1148 and 1108 cm⁻¹ in curves b, c, and d corresponding to ν_3 SO₄²⁻ stretching, and it exhibits a small red shift in comparison to that of HH whiskers in absent of ethylene glycol, where the bands appear at 1154 and 1112 cm⁻¹. These changes suggest that ethylene glycol interacts strongly with the SO₄²⁻ group, and probably form hydrogen bonds.

Figure 9 shows the schematic drawing of the growth mechanism of HH whiskers. The adsorption of ethylene glycol on the side facets of HH whiskers as (200), (220), and (400) inhibited the growth on these facet, which favored the selective growth of the whiskers along the *c* axis and promoted the formation of HH whiskers with high aspect ratio. However, with the increasing concentration of ethylene glycol, the ethylene glycol would absorb on the surface of two different whiskers, and lower the aspect ratio (as insert enlarged image shown in figure 1d).

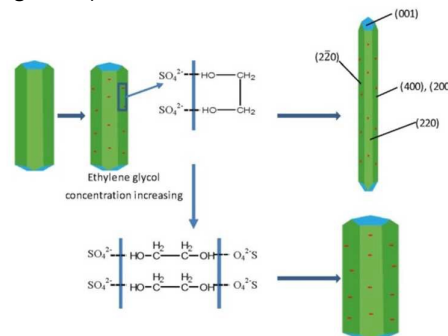


Figure 9. Schematic drawing of adsorption of ethylene glycol on HH whiskers

Conclusions

A facile ethylene glycol-assisted hydrothermal method was developed to synthesis HH whiskers with high aspect ratios. The presence of 3.76×10^{-3} mol·L⁻¹ ethylene glycol led to the aspect ratio of HH whiskers up to 400. Further increased concentration of ethylene glycol would lower the aspect ratio. The adsorption of ethylene glycol on the side surfaces of HH whiskers as (200), (220), and (400) inhibited the growth of these facets and promoted the 1-D growth of HH whiskers along the *c* axis.

Acknowledgements

This work is supported by the National Natural Science Foundation of China (21306094) and Promotive research fund for excellent young and middle-aged scientists of Shandong Province (J13LD15).

Notes and references

- 1 Lv, J. Qiu, L. Z. Qu, B. J. *Nanotechnology* 15 (11): 1576-1581 (2004).
- 2 M. Nath and B. A. Parkinson, *Adv. Mater.* 18 (14), 1865 (2006).
- 3 Li SY, Lee CY, Lin P, Tseng TY *Nanotechnology* (2005) 16:451-457.
- 4 Kim H W, Shim S H.. *Chem.Phys.Lett.*, 2006, 422: 165-169.
- 5 Y.J. Chen, J.B. Li, Y.S. Han, X.Z. Yang, J.H. Dai, *J. Cryst. Growth* 245 (2002) 163.
- 6 [6] Mituhashi K, Tagami N, Tanabe K, et al. *Langmuir*, 2005, 21 : 3659-3663.
- 7 Eshelby. *J. Solid State Phys.* 1956, 3, 79-144.
- 8 Gurtin, M. E.; Murdoch, A. I. *Arch. Ration. Mech. Anal.* 1975, 57, 291-323.
- 9 Bacon, D.; Barnett, D.; Scattergood, R. O. *Prog. Mater. Sci.* 1980, 23, 51-262.
- 10 Xingfu Song*, Lina Zhang, Jingcai Zhao, Yanxia Xu, Ze Sun, Ping Li, and Jianguo Yu. *Cryst. Res. Technol.*, 2011,46 (2):166 – 172
- 11 [11] Li LY, Li B, Yang GL, Li CY. *Langmuir* 2007, 23(16):8522-8525.
- 12 Li WG, Xu LL, Dai J. *J Synth Cryst* 2005,34(2):323-327.
- 13 Shi PY, Deng ZZ, Yuan YY, Sun J. *J Northeast Univ (Nat Sci)* 2010, 31(1):76-79.
- 14 Wang SL, Jiang XY, Chen FS, Chen XX. *J Qingdao Univ Sci Technol (Nat Sci Ed)* 2010, 31(4):376-379.
- 15 Lee EJ, Jeon SH, Chae JH, Heo JW, Kang K, Kim J, Kim KP, Lee KW. *Tissue Eng Regen Med* 2009 , 6(1-3):287-293
- 16 Wang HG, Mu B, Ren JF, Jian LQ, Zhang JY, Yang SR . *Polym Compos* 2009, 30(9):1326-1332.
- 17 Tang M, Shen X, Huang H. *Mater Sci Eng* 2010, 30(8):1107-1111.
- 18 Liu JY. *Express Polym Lett* 2011, 5(8):742-752.
- 19 Murariu, M.; Da Silva Ferriera, A.; Degée; Alexandre, M.; Dubois, *Polymer* 2007, 48, 2613-2618.
- 20 Hou, S; Wang, J; Wang, X; Chen, H; Xiang, L. *Langmuir*. 2014,30(32), 9804-9810.
- 21 Hou, S.; Xiang, L. *J. Nanomater.* 2013, 2013.
- 22 Hua He, Faqin Dong, Ping He, Longhua Xu. *J Mater Sci* (2014) 49:1957-1963
- 23 Kong, B.; Guan, B.; Yates, M. Z.; Wu, Z. *Langmuir* 2012, 28, 14137-14142.
- 24 Fan, X. B.; Peng, W. C.; Li, Y.; Li, X. Y.; Wang, S. L.; Zhang, G. L.; Zhang, F. B. *Adv. Mater.* 2008, 20, 4490-4493.
- 25 Moulder, J. F.; Stickle, W. F.; Sobol, P. E.; Bomben, K. D. *Handbook of X-ray photoelectron spectroscopy*; Perkin-Elmer Corporation: Eden Prairie, MN, 1992.
- 26 *Material Studio 5.0*, developed by Molecular Simulations Inc.(MSI), Genetics Computer Group(GCG), Synopsys Scientific and Oxford Molecular Group(OMG) in 2009.
- 27 Ballirano, P.; Maras, A.; Meloni, S.; Caminiti, R. *Eur. J. Mineral* 2001, 13, 985-993.
- 28 Bezou, C.; Nonat, A.; Mutin, J. C. *J. Solid State Chem.* 1995, 117, 165-176.
- 29 Freyer, D.; Voigt, W. *Monatsh. Chem.* 2003, 134, 693-719.
- 30 Anto PL, Anto RJ, Varghese HT, Panicker CY, Philip D, Brolo AG (2009) FT-IR. *J Raman Spectrosc* 40(12):1810-1815.
- 31 Sutter B, Dalton JB, Ewing SA, Amundson R, McKay CP (2007). *J Geophys Res Biogeosci* 112 (G4).